HHS Public Access

Author manuscript

Sci Signal. Author manuscript; available in PMC 2025 July 23.

Published in final edited form as:

Sci Signal. 2024 July 23; 17(846): eadh2381. doi:10.1126/scisignal.adh2381.

The kinase ITK controls a Ca^{2+}-mediated switch that balances T_H17 and T_{reg} cell differentiation

Orchi Anannya[1], **Weishan Huang**[1,2], **Avery August**[1,3,4,5,*]

[1]Department of Microbiology and Immunology, College of Veterinary Medicine, Cornell University, Ithaca, NY, 14853, USA

[2]Department of Pathobiological Sciences, School of Veterinary Medicine, Louisiana State University, Baton Rouge, LA 70803, USA

[3]Cornell Center for Immunology, Cornell University, Ithaca, NY 14853, USA

[4]Cornell Institute of Host-Microbe Interactions and Disease, Cornell University, Ithaca, NY 14853, USA

[5]Cornell Center for Health Equity, Cornell University, Ithaca, NY 14853, USA

Abstract

The balance of proinflammatory T helper type 17 (T_H17) and anti-inflammatory T regulatory (T_{reg}) cells is crucial for immune homeostasis in health and disease. The differentiation of naïve $CD4^+$ T cells into T_H17 and T_{reg} cells depends upon T cell receptor (TCR) signaling mediated in part by interleukin-2–inducible T cell kinase (ITK), which stimulates mitogen-activated protein kinases (MAPKs) and Ca^{2+} signaling. Here, we report that, in the absence of ITK activity, naïve murine $CD4^+$ T cells cultured under T_H17-inducing conditions expressed the T_{reg} transcription factor Foxp3 and did not develop into T_H17 cells. Furthermore, ITK inhibition in vivo during allergic inflammation increased the T_{reg}:T_H17 ratio in the lung. These switched $Foxp3^+$ T_{reg}-like cells had suppressive function, and their transcriptomic profile resembled that of differentiated, induced T_{reg} (iT_{reg}) cells, but their chromatin accessibility profiles were intermediate between T_H17 and iT_{reg} cells. Like iT_{reg} cells, switched $Foxp3^+$ T_{reg}-like cells had reductions in the

*Corresponding author. averyaugust@cornell.edu.

Author contributions:
Conceptualization: AA, WH
Methodology: OA, WH
Investigation: OA, WH
Visualization: OA, WH, AA
Funding acquisition: AA, WH
Project administration: AA
Supervision: AA
Writing – original draft: OA, AA
Writing – review & editing: OA, WH, AA

Competing interests:
A.A. declares research funding from the 3M Company. The other authors declare that they have no competing interests.

Data and materials availability:
RNA-Sequencing and ATAC-Seq data have been deposited into the Gene Expression Omnibus repository of the National Center for Biotechnology Information (NCBI: https://www.ncbi.nlm.nih.gov/geo/) with the accession numbers GSE261352 and GSE266002, respectively. RNA-Sequencing GEO data for Tr1, pT_H17, npT_H17, T_H1 and T_H2 were from GSE158703. All other data needed to evaluate the conclusions in the paper are present in the paper or the supplementary materials.

expression of genes involved in mitochondrial oxidative phosphorylation and glycolysis, in the activation of the mechanistic target of rapamycin (mTOR) signaling pathway, and in the abundance of the T_H17 pioneer transcription factor BATF. This ITK-dependent switch between T_H17 and T_{reg} cells depended on Ca^{2+} signaling but not on MAPKs. These findings suggest potential strategies for fine-tuning TCR signal strength through ITK to control the balance of T_H17 and T_{reg} cells.

INTRODUCTION

Immune function mediated by T helper (T_H) cells is critical for the development of effective barriers to pathogens and environmental toxins. Distinct functions are mediated by specific lineages of T_H cells that have generally proinflammatory functions (such as the T_H1, T_H2, T_H9, and T_H17 lineages) or anti-inflammatory functions (such as cells of the T regulatory (T_{reg}) and type 1 T_{reg} (Tr1) lineages). These distinct T_H cell lineages are characterized by the expression of lineage-specific transcription factors and effector cytokines that mediate immune responses (1). T_H17 cells are characterized by expression of the transcription factor RORγt (RAR-related orphan receptor gamma), and produce the effector cytokines interleukin-17A (IL-17A), IL-17F, IL-21, and IL-22 in response to infection with extracellular bacteria, parasites, or allergens (1). T_{reg} cells are characterized by expression of the transcription factor Forkhead box P3 (Foxp3) and produce effector cytokines, such as IL-10 and transforming growth factor β (TGF-β), that can suppress the function of T_H1, T_H2, T_H9, T_H17, and other immune cells (1).

The commitment of naïve $CD4^+$ T cells to generally proinflammatory T_H17 effector fates, or to generally anti-inflammatory $Foxp3^+$ T_{reg} fates, depends on the strength of T cell receptor (TCR) signaling and the cytokines present in the microenvironment (2–6). Key events include triggering of TCR signals upon interaction with antigen-major histocompatibility complex (MHC) complexes and subsequent recruitment of the Src family kinases Lck and Fyn and the Syk family kinase ZAP-70 (zeta chain–associated kinase), which phosphorylates the adaptor proteins LAT (linker for activation of T cell) and SLP76 (SH3 containing lymphocyte protein 76) (7, 8). This is followed by assembly of a proximal signaling complex that includes the recruitment of interleukin-2–inducible T cell kinase (ITK) and SLP76 (7, 8). ITK functions in part by activating PLCγ (phospholipase Cγ) to generate the effector molecules IP_3 (inositol triphosphate) and DAG (diacylglycerol) (7–9). This allows the activation of MAPK (mitogen-activated protein kinase) cascades, enhanced cytosolic Ca^{2+} concentrations required to activate NFAT (nuclear factor of activated T cells), and the activation of mTOR (mechanistic target of rapamycin) by the kinase Akt (8). TCR signal strength is positively regulated by ITK, with higher ITK activity providing stronger signals downstream of the TCR (8). The initial stages of T cell activation depend on TCR activation and the presence of select cytokines in the microenvironment, and once activated, T cells undergo further metabolic changes unique to each T cell subset (10). These metabolic changes allow maintenance and function of specific T cell subsets; for example, T_H17 cells depend on mitochondrial oxidative phosphorylation and glycolysis (11, 12). These metabolic changes in turn regulate expression of key molecules that allow function of these T cell subsets as proinflammatory T_H17 or anti-inflammatory T_{reg} cells (10).

Given the critical role of ITK in regulating the development and function of T cell lineages, several studies have investigated the function of ITK in the development of different immune responses. We and others have also shown that the absence of ITK or ITK activity in naïve $CD4^+$ T cells impaired the differentiation into T_H2, T_H9, T_H17 and Tr1 lineages, and enhanced the differentiation into T_H1 and T_{reg} lineages (13–18). TCR signal strength mediated by ITK plays an important role in T_H17 and T_{reg} cell differentiation (14, 17, 19), and we sought to determine whether inhibition of ITK regulates T_H17 and T_{reg} lineage commitment, and the mechanisms by which these events are controlled.

Here, we investigated this by using ITK inhibitors and mice expressing allele-sensitive forms of ITK (ITK*as*), which enables the selective inhibition of ITK in these mice with ITK*as*-selective inhibitor compounds (16, 20–23). Under conditions that promote Th17 differentiation, inhibition of ITK suppressed naïve $CD4^+$ T cell differentiation to the T_H17 lineage, and instead led to the generation of $Foxp3^+$ T_{reg}-like cells. The resultant population of $Foxp3^+$ T_{reg}-like cells expressed markers associated with T_{reg} cells, effectively retained expression of the T_{reg} transcription factor Foxp3, and demonstrated effective suppression of T cell proliferation responses. Furthermore, inhibition of ITK in vivo during allergic inflammation also led to higher lung T_{reg};T_H17 ratios. The switched $Foxp3^+$ T_{reg}-like cells had T_{reg}-like transcriptomic and chromatin accessibility profiles. Switched $Foxp3^+$ T_{reg} cells also resembled inducible T_{reg} cells (iT_{reg} cells) in that they displayed reduced expression of key genes and markers involved in mitochondrial oxidative phosphorylation and glycolytic pathways. This apparent overall reduction in oxidative phosphorylation was associated with reduced phosphorylation of mTOR and its downstream substrate S6K (ribosomal S6 kinase), which may act to prevent expression of the T_H17 pioneer transcription factor BATF (basic leucine zipper ATF-like transcription factor). Finally, we show that bypassing the TCR signal to increase Ca^{2+} signaling prevented this ITK-dependent switch response. Our results indicate that ITK signals can tune the balance between T_H17 cells and T_{reg} cells.

RESULTS

ITK controls a switch between T_H17 and $Foxp3^+$ T_{reg}-like cells during T_H17 differentiation

Because the absence of ITK in naïve $CD4^+$ T cells inhibits T_H17 differentiation and induces the appearance of T cells expressing $Foxp3^+$ (14–17), we investigated whether ITK activity loss causes a switch from T_H17 to T_{reg} differentiation. To determine the role of ITK activity in the development of $Foxp3^+$ T_{reg} cells under T_H17 conditions, we isolated naïve T cells from wild-type (WT), *Itk*$^{-/-}$, or ITK*as* IL-17A-GFP/Foxp3-RFP reporter mice. In these reporter mouse strains, the genes encoding green fluorescent protein (GFP) and red fluorescent protein (RFP) are inserted downstream of an internal ribosome entry sequence (IRES) in the *Il17a* and *Foxp3* loci, respectively, which allows the endogenous protein and the fluorescent reporter protein to be expressed from the same mRNA (16,18,46). These naive WT, *Itk*$^{-/-}$, or ITK*as* IL-17A-GFP/Foxp3-RFP reporter T cells were stimulated with anti-CD3 and anti-CD28 antibodies presented by antigen-presenting cells (APCs, adherent macrophages and dendritic cells collected from the spleens of *Rag1*$^{-/-}$ mice), in the presence of recombinant IL-6, TGF-β, and human IL-2, hereafter referred to as T_H17 culture conditions. To inhibit WT ITK, we used the small-molecule compound CPI-818

which irreversibly inhibits ITK kinase activity by covalently binding to residue Cys^{442} within the active site and has 100 fold greater selectivity for ITK (IC_{50} = 2.3 nM) relative to related Tec kinase Rlk (430 nM) and BTK (850 nM) (23–25). To inhibit ITK*as*, we used 3MBPP1 (IC_{50} ~50 nM) which has >400 fold selectivity compared to WT ITK and related Tec kinases Rlk and Tec (16). We found that the absence of ITK or inhibition of ITK*as* with 3MBPP1 resulted in the suppression of IL-17^+ T_H17 cell differentiation and the appearance of Foxp3^+ T_{reg}-like cells (Fig. 1A). Similarly, stimulation of naïve WT IL-17A-GFP/Foxp3-RFP reporter T cells under T_H17 culture conditions in the presence of CPI-818 (23) resulted in dose-dependent inhibition of T_H17 cell differentiation, along with the appearance of Foxp3^+ T_{reg}-like cells (Fig. 1B). Inhibiting ITK did not result in the appearance of IL-$17A^+$/Foxp3^+ T cells (Fig. 1, A and B; fig. S1, A and B). This effect was due to specific inhibition of ITK and not potential off-target effects because the covalent small molecule ITK inhibitor CPI-818 did not affect T_H17 differentiation of naïve ITK*as* T cells, nor did 3MBPP1 affect T_H17 differentiation of naïve WT T cells (fig. S1, A and B). We refer to these Foxp3^+ T_{reg}-like cells generated under conditions of ITK inhibition as "switched Foxp3^+ T_{reg}-like" cells.

ITK inhibition does not switch differentiated T_H17 cells to Foxp3^+ T_{reg}-like cells

To determine whether inhibition of ITK can induce differentiated T_H17 cells to switch to become Foxp3^+ T_{reg}-like cells, we generated T_H17 cells and in vitro–switched Foxp3^+ T_{reg}-like cells, sorted them, then cultured the sorted cells under T_H17 differentiation conditions in presence of the covalent ITK inhibitor CPI-818. Whereas there was no change in the switched Foxp3^+ T_{reg}-like cells, inhibiting ITK led to a reduction in differentiated T_H17 cells (Fig. 1C), suggesting that ITK activity is required for the maintenance of these cells. However, inhibiting ITK in these T_H17 cells did not lead to the development of Foxp3^+ T_{reg}-like cells under these conditions (Fig. 1C). These data suggest that, under T_H17 differentiation conditions, inhibition of ITK switches T_H17 differentiation to Foxp3^+ T_{reg}-like cells but does not switch cells that have already differentiated to the T_H17 fate.

Early events following TCR activation determine the capacity of ITK to tune a switch from T_H17 to Foxp3^+ T_{reg}-like cells

To determine if early or late molecular events influenced this switch to Foxp3^+ T_{reg}-like cells upon ITK inhibition, naïve WT $CD4^+$ T cells were activated under T_H17 differentiation conditions, followed by addition of the ITK inhibitor CPI-818 at 1, 2, 3, or 4 days after the initiation of differentiation. We found that inhibition of ITK blocked T_H17 differentiation only when added within the first 2 days of culture (Fig. 2A). The generation of switched Foxp3^+ T_{reg}-like cells also showed a time-dependent relationship between ITK inhibition and the appearance of these cells, although optimal generation required early ITK inhibition, because ITK inhibition at later time points beyond day 1 was less effective in inducing the switch, with some Foxp3^+ T_{reg}-like cell generation upon ITK inhibition on day 2, and no significant effect upon ITK inhibition between days 3 to 5 (Fig. 2A).

Next, we wanted to determine the time frame of ITK inhibition that results in this switch response. Using a similar approach, naïve WT $CD4^+$ T cells were activated under T_H17 differentiation conditions in the presence of CPI-818, followed by removal of the inhibitor

after 1, 2, 3, or 4 days. The presence of CPI-818 for 1 day led to an ~50% inhibition of T_H17 cell differentiation, but the greatest effect was observed with 5 days of ITK inhibition (Fig. 2B). Analogously, the generation of switched Foxp3$^+$ T_{reg}-like cells was observed when ITK was inhibited for as little as 1 day (~40% of maximal generation), and close to maximum after 3 days of ITK inhibition (Fig. 2B). Taken together, this suggests that early events following TCR activation determines the switch from T_H17 to switched Foxp3$^+$ T_{reg}-like cells upon ITK inhibition.

Switched Foxp3$^+$ T_{reg}-like cells resemble true Foxp3$^+$ T_{reg} cells and can suppress naïve T cell proliferation in vitro

In addition to expression of Foxp3, T_{reg} cells express a number of cell surface molecules including CD25, CTLA4 (cytotoxic T-lymphocyte associated protein 4), and PD1 (programmed cell death protein 1) (1). To determine if the switched Foxp3$^+$ T_{reg}-like cells, generated upon ITK inhibition of naïve CD4$^+$ T cells cultured under T_H17 conditions, resembled true T_{reg} cells, we compared the expression of these cell surface markers by flow cytometry. We found that all T_{reg} subsets [in vitro–generated induced T_{reg} cells (iT_{reg} cells), thymic-derived natural T_{reg} cells (T_{reg} cells), and extra-thymic peripheral T_{reg} cells (pT_{reg} cells), and the switched Foxp3$^+$ Treg-like cells] expressed CD25, CTLA4, and PD1, with switched Foxp3$^+$ T_{reg}-like cells most closely resembling the iT_{reg} cells in their expression of these markers (Fig. 3A). Subsequently we investigated if the switched Foxp3$^+$ T_{reg}-like cells were able to suppress the proliferation of carboxyfluorescein succinimidyl ester (CFSE)-labeled naïve CD4$^+$ T cells when cocultured in vitro. In the absence of coculture with T_{reg} cells, responding naïve T cells undergo multiple rounds of cell division when activated by anti-TCR antibodies, as determined by CFSE dye dilution (Fig. 3B). However, when cocultured in presence of iT_{reg} cells, this proliferation was suppressed (Fig. 3B). In presence of the switched Foxp3$^+$ T_{reg}-like cells, similar to the iT_{reg} cells, this proliferation of responding T cells was also suppressed (Fig. 3B). Therefore, the switched Foxp3$^+$ T_{reg}-like cells expressed surface markers and displayed suppressive function similar to iT_{reg} cells.

ITK controls the Foxp3$^+$ T_{reg}:T_H17 cell ratio in the lung during allergic airway inflammation

To determine whether ITK plays a role in the balance of T_H17 and Foxp3$^+$ T_{reg} cells in vivo, we examined a mouse model of house dust mite (HDM)–induced allergic airway inflammation, which induces the development of T_H17 and Foxp3$^+$ T_{reg} cells (26). WT IL7A-GFP/Foxp3-RFP mice were exposed intranasally to HDM extract for 10 days, followed by a second round of 10-day intranasal exposure to HDM extract along with treatment with ITK inhibitor CPI-818 or vehicle, followed by analysis of lung cells for T_H17 and Foxp3$^+$ T_{reg} cells. We found that treatment with CPI-818 significantly reduced the percentage of T_H17 cells in the lungs, with no significant change in the percentage of Foxp3$^+$ T_{reg} cells (Fig. 3C), along with reduced total lung cells and total lymphocytes, and a trend toward reduced neutrophils but not eosinophils (fig. S2A). In order to determine whether the reduced T_H17 responses observed with ITK inhibition after the development of HDM- induced inflammation was specifically due to ITK inhibition and not off-target effects, we treated mice expressing the ITK*as* (instead of WT ITK) with the WT ITK inhibitor CPI-818. ITK*as* IL-17-GFP/Foxp3-RFP reporter mice were exposed to HDM as described above with simultaneous treatment with the WT ITK inhibitor CPI-818 for the

second round of exposure. Treatment of ITK*as* mice with the WT ITK inhibitor CPI-818 did not affect the percentage of T_H17 cells, the percentage of T_{reg} cells, the ratio of percent of Foxp3$^+$ T_{reg}:T_H17 cells in the lungs (Fig. 3D), or total lung cells, total lymphocytes, neutrophils, or eosinophils (fig. S2B), confirming the specificity of this response.

The transcriptome of switched Foxp3$^+$ T_{reg}-like cells resembles that of iT_{reg} cells

We next investigated the transcriptomic profile of the switched Foxp3$^+$ T_{reg}-like cells, comparing them to T_H17 cells and iT_{reg} cells, using RNA-Sequencing (RNA-Seq) analysis of cells differentiated in vitro from WT naïve CD4$^+$ T cells. Principal component analysis (PCA) and heatmap analysis displaying expression of all transcripts, indicated that the switched Foxp3$^+$ T_{reg}-like cells more closely resembled iT_{reg} cells than they did T_H17 cells (Fig. 4A and B). Using volcano plots to identify differentially expressed transcripts, we found that those coding for the T_H17 cytokine IL-17 (*Il17)* and the critical T_H17 transcription factor RORγt (*Rorc*) were reduced in switched Foxp3$^+$ T_{reg}-like cells compared to T_H17 cells (Fig. 4C). Furthermore, *Foxp3* and other T_{reg}-related transcripts, such as *Tgfbr1* and *Tgfbr2*, as well as those encoding other transcription factors (*Smad3* and *Ikzf2*) were increased in switched Foxp3$^+$ Treg-like cells compared to T_H17 cells (Fig. 4C). The T_H17 cells expressed genes encoding the expected complement of IL-17-related cytokines (*Il17a, Il17f*, and *Il22*), but switched Foxp3$^+$ T_{reg}-like cells did not express *Il10*, and switched Foxp3$^+$ T_{reg}-like cells derived from IL-10-GFP/Foxp3-RFP reporter mice did not express IL-10-GFP (fig. S3, A and B). The switched Foxp3$^+$ T_{reg}-like cells also expressed lower amounts of Treg-related genes *Foxp3, Nrp1, Tgfb1*, and *Tgfbr1* but higher amounts of *Tgfb3* (Fig. 4C).

To compare the transcriptomes of switched Foxp3$^+$ T_{reg}-like cells with other T cell subsets, we compared their transcriptomes to transcriptomic data from T_H1, T_H2, and pathogenic T_H17 (pT_H17) cells generated in the presence of IL-1β, IL-6, and IL-23, from nonpathogenic T_H17 (npT_H17) cells generated in presence of IL-6 and TGF-β, and from Tr1 cells (GSE158703)(27). We found that the transcriptome of switched Foxp3$^+$ T_{reg}-like cells, T_H17, and iT_{reg} subsets we generated clustered closer to the npT_H17 and pT_H17 subsets, and further from T_H1 and T_H2 subsets, with Tr1 cells being furthest in the cluster comparison (Fig. 4D).

The chromatin profile of switched Foxp3$^+$ T_{reg}-like cells is distinct from both T_H17 and iT_{reg} cells

We also analyzed chromatin accessibility in switched Foxp3$^+$ T_{reg} cells by ATAC-Seq (assay for transposase-accessible chromatin using sequencing), comparing them to T_H17 and iT_{reg} cells. Analysis by PCA and heatmaps revealed that, similar to the transcriptomic analysis, switched Foxp3$^+$ T_{reg}-like cells had chromatin profiles that more closely resembled iT_{reg} cells than T_H17 cells (Fig. 5A and B). Using volcano plots to compare differentially open and closed chromatin regions, we found that the chromatin region of genes associated with T_H17 cells (for example, *Rora, Stat3, Il17, Foxp1*) displayed reduced accessibility in switched Foxp3$^+$ T_{reg}-like cells compared to T_H17 cells (Fig. 5C). By contrast, the chromatin regions of genes associated with iT_{reg} cells (for example, *Il10rb, Tgfbr3*) displayed reduced accessibility in switched Foxp3$^+$ T_{reg}-like cells compared to iT_{reg}

cells (Fig. 5C), whereas the T_H17-related gene *Rora* was more open, perhaps reflecting relatedness to T_H17 cells (Fig. 5C). Individual chromatin region traces depict these differences, where switched Foxp3$^+$ T_{reg}-like display reduced accessibility for T_H17 genes (*Rorc, Il17*) but enhanced accessibility for genes associated with iT_{reg} cells (*Foxp3*) (Fig. 5D).

Enhanced Ca^{2+} signaling prevents the ITK inhibition–dependent switch to Foxp3$^+$ T_{reg}-like cells

The differentiation of naïve CD4$^+$ T cells into T_H17 cells depends on the presence of cytokines and TCR activation. An important component downstream of TCR activation and ITK signaling is Ca^{2+} signaling, and increased intracellular Ca^{2+} rescues the development of T_H17 cells in the absence of ITK (14). To determine whether this pathway downstream of ITK is important for the ITK inhibition–dependent switch response, we used ionomycin to increase cytosolic Ca^{2+} concentrations during T_H17 differentiation conditions in the presence of ITK inhibition. In the absence of ITK (using naïve *Itk*$^{-/-}$ CD4$^+$ T cells), T_H17 differentiation was prevented, and this was rescued by ionomycin treatment (Fig. 6A), confirming the role of the Ca^{2+} pathway in T_H17 differentiation downstream of ITK. In addition, ionomycin prevented the switch to Foxp3$^+$ T_{reg}-like cells (Fig. 6A), indicating a critical role for the Ca^{2+} pathway in tuning this switch. To examine if this was also observed with ITK inhibition, we increased cytosolic Ca^{2+} with ionomycin during T_H17 differentiation conditions in the presence of the ITK inhibitor CPI-818. Increasing intracellular Ca^{2+} enhanced T_H17 differentiation and rescued T_H17 differentiation when ITK was inhibited (Fig. 6B). Together these results indicate that increases in intracellular Ca^{2+} signaling under T_H17 differentiation conditions promoted the generation of T_H17 cells and suppressed the generation of switched Foxp3$^+$ T_{reg}-like cells in the absence of ITK activity. When naïve CD4$^+$ T cells were cultured under iT_{reg} conditions, the loss of ITK (*Itk*$^{-/-}$ cells) or inhibition of ITK activity increased the differentiation of iT_{reg} cells, and increasing intracellular Ca^{2+} with ionomycin suppressed the differentiation of iT_{reg} cells and caused some differentiation of T_H17 cells (Fig. 6, C and D) (17). To confirm that absence of Ca^{2+} promoted the generation of switched Foxp3$^+$ T_{reg}-like cells, we used thapsigargin, which increases cytosolic Ca^{2+}, with or without the ITK inhibitor CPI-818. We found that thapsigargin also increased T_H17 differentiation and reduced the switched Foxp3$^+$ T_{reg}-like cell generation in the presence of ITK inhibition (fig. S4A).

The TCR-induced activation of the ITK-PLCγ1 axis generates IP_3 and DAG, the latter of which can activate Ras guanyl nucleotide–releasing protein 1 (RasGRP1), leading to the activation of Ras, Raf, and the MAPKs (mitogen activated protein kinases) JNK (c-Jun N-terminal kinase), p38, and ERK (extracellular signal–regulated kinase) (28). Our results described above indicated a critical role for the Ca^{2+} pathway, emanating from the generation of IP_3, in the ITK inhibition–dependent switch from T_H17 to Foxp3$^+$ T_{reg}-like cells. To determine whether the DAG pathway plays a role in this process, we examined MAPK pathways downstream of Ras regulated by DAG- activated RasGRP1. We used inhibitors of Raf, JNK, p38, and ERK to inhibit activation of these kinases during T_H17 differentiation conditions. We found that inhibition of these kinases had differential effects on T_H17 differentiation (inhibition of JNK, but not inhibition of ERK, p38, or Raf, reduced

T_H17 differentiation), but did not induce the generation of switched Foxp3$^+$ T_{reg}-like cells, as was observed in the absence of ITK or its activity (fig. S4B, and compare to Fig. 1). Furthermore, the inclusion of PMA (phorbol 12-myristate 13-acetate, a DAG mimic that activates Ras), during T_H17 differentiation did not affect T_H17 differentiation, but did reduce the appearance of switched Foxp3$^+$ T_{reg}-like cells induced upon ITK inhibition by CPI-818 (fig. S4C). Taken together, these results suggest that the negative regulation of T_{reg} differentiation, and more broadly, tuning of T_H17 and T_{reg} differentiation by ITK is mediated partly by Ca^{2+} signaling.

ITK–dependent switching is associated with deficits in molecules involved in mitochondrial oxidative phosphorylation and reduced expression of BATF

Specific sets of genes are associated with pathogenic T_H17 cells and nonpathogenic T_H17 cells (29, 30). By comparing the expression of these select genes in our RNA-Seq data, we found that switched Foxp3$^+$ T_{reg}-like cells were distinct from T_H17 cells and instead resembled iT_{reg} cells (Fig. 7A). Several metabolic changes are also associated with T_H17 cell development, and thus we compared the expression of select genes involved in these pathways during T_H17 cell development (29, 30). For genes that are associated with tricarboxylic acid (TCA) cycle activity and mitochondrial function, switched Foxp3$^+$ T_{reg}-like cells displayed expression patterns distinct from T_H17 cells and instead resembled iT_{reg} cells (Fig. 7A). In contrast, for genes that are associated with the hypoxia-induced factor (HIF) pathway and glycolysis, switched Foxp3$^+$ T_{reg}-like cells resembled T_H17 cells but not iT_{reg} cells (Fig. 7A). Therefore the switched Foxp3$^+$ T_{reg}-like cells had an intermediate metabolic phenotype, resembling in part both the T_H17 and iT_{reg} metabolic phenotypes.

We next examined the cells for evidence of activation of select molecules involved in the pathways of mitochondrial oxidative phosphorylation (29), by estimating the phosphorylation status of mTOR and S6K (ribosomal S6 kinase), because their activation is involved in determining T_H17 states. Using flow cytometric analysis of naïve CD4$^+$ T cells cultured under T_H17 differentiation condition either with or without the ITK inhibitor CPI-818, we found reduced phosphorylation of S6K and mTOR in CD4$^+$ T cells when ITK activity was inhibited compared to control conditions, suggesting reduced mitochondrial oxidative phosphorylation upon ITK inhibition (Fig. 7B, fig. S3C).

The transcription factor BATF is a pioneer transcription factor for T_H17 differentiation and is involved in early events during T_H17 differentiation (29). We found that inhibition reduced the percentage of CD4$^+$ T cells that were both RORγt$^+$ and BATF$^+$, and further analysis by gating on just the RORγt$^+$ cells followed by analysis of BATF expression indicated reduced BATF expression under T_H17 conditions when ITK's activity was inhibited compared to control (Fig. 7C). We also found reduced mRNA expression (Fig. 7D) and reduced chromatin accessibility for *Batf, Batf2*, and *Batf3* in the switched Foxp3$^+$ T_{reg}-like cells compared to the T_H17 and iT_{reg} cells (Fig. 7E). Taken together, we demonstrated that ITK inhibition under T_H17 differentiation conditions lead to deficits in molecules that mediate mitochondrial oxidative phosphorylation and reduced the expression of BATF, which may be involved in the ITK inhibition–dependent switch to Foxp3$^+$ T_{reg}-like cells under T_H17 differentiation conditions.

DISCUSSION

The capacity of TCR signals to control the differentiation of T_H17 and T_{reg} cells has been a focus of intense study because a better understanding of this process may provide approaches for differential regulation of these T effector subsets in specific immune responses and autoimmune disease. We demonstrate here that the tyrosine kinase ITK tunes a switch between T_H17 cells and Foxp3$^+$ T_{reg} cells, and that is mediated by Ca^{2+} signaling and associated with altered cellular metabolism, involving at least in part reduced mTORC signaling with BATF functioning as one of the downstream components. Our findings provide substantial mechanistic understanding of how ITK regulates T_H17 cells and T_{reg} cells (Fig. 7F) (14, 19, 31) and suggest that ITK signaling may control inflammation and anti-inflammation during activation of naïve CD4$^+$ T cells. Our work further shows that this ITK-mediated tuning of T_H17 and T_{reg} cell fates requires specific signals from ITK during the initial 24–48 hr. period of activation under T_H17 conditions, indicating early molecular events regulate the switch response.

In this study, we found that switched Foxp3$^+$ T_{reg}-like cells resembled iTr_{eg} cells not only in their expression of Foxp3 but also in terms of their phenotypic profile based on the expression of T_{reg} markers CD25, CTLA4, and PD1, as well as suppressive function in vitro. Foxp3 is critical for the development and function of T_{reg} cells; however, there are also reports that expression of Foxp3 alone was not sufficient for T_{reg}-mediated suppressive function (32, 33). Other reports show that the amount of Foxp3 and CD45R protein within human lymphocytes defined a heterogenous T_{reg} population wherein each T_{reg} subset varied in both phenotype and function (32, 33). In addition to select phenotypic markers, several studies have utilized comparison of the whole transcriptome and epigenetic landscape to compare T cell subsets. Whereas the transcriptome allowed clear demarcations of phenotypic profile of genes expressed in each T cell subset, investigation into chromatin accessibility status provided a more nuanced view of these cellular states between the different T cell subsets. Although the T_H17 cells expressed the expected complement of IL-17–related cytokines IL-17A, IL-17F, and IL-22, the switched Foxp3 T_{reg}-like cells did not express the T_{reg} cytokine IL-10. Comparing the chromatin profile of the *Foxp3* locus by ChIP-Seq, for example, has revealed that selective activating histone modifications exist in iT_{reg} cells and not in T_H1 or T_H2 cells, but that these activating marks were also present in T_H17 cells, indicating some similarities in overall chromatin structure shared by iT_{reg} cells and T_H17 cells (34). That study also suggested that the chromatin landscape of in vitro–derived T cells display considerable plasticity, because when studying the locus of the gene encoding the T_H2 transcription factor Gata3, it was reported that in order to achieve full activation status and associated histone modifications, two rounds of T_H2 polarization were required instead of a single T_H2 polarization period (34). These observations may explain the discrepancy we observed between transcriptomes and the chromatin accessibility profile. Thus, the switched Foxp3$^+$ T_{reg}-like cells appear to have attained the transcriptomic profile of iT_{reg} cells, but further rounds of polarization may be required to induce full transition to the iT_{reg} chromatin accessibility profile.

We and others have reported that ITK functions to fine-tune TCR signal strength, being a positive regulator for T_H1, T_H17, and Tr1 cells but a negative regulator for T_H2 and

iT_{reg} cells. Several studies report that increasing the TCR signal strength enhanced the differentiation of naïve $CD4^+$ T cells into T_H17 cells under T_H17 polarization conditions but inhibited the differentiation of naïve $CD4^+$ T cells into iT_{reg} cells under iT_{reg} polarization conditions (14, 15, 35–38). Increased TCR signaling is associated with enhanced Ca^{2+} signaling (39, 40) and we and others have demonstrated that increasing Ca^{2+}-dependent calmodulin and NFATc1 signaling restores T_H17 differentiation of naïve *Itk*$^{-/-}$ $CD4^+$ T cells polarized under T_H17 conditions (14, 15, 38). The findings of the present study show that increasing Ca^{2+} enhanced T_H17 differentiation in naïve $CD4^+$ T cells also rescued T_H17 differentiation when ITK activity was inhibited. Furthermore, increased Ca^{2+} not only prevented the switch to $Foxp3^+$ T_{reg}-like cells with ITK inhibition under T_H17 conditions but also prevented the increased iT_{reg} differentiation with ITK inhibition under iT_{reg} polarization condition, suggesting that the Ca^{2+}-regulated pathway is a key regulator of these two fates.

Ca^{2+} signaling was previously reported to control mitochondrial metabolism, and deletion of stromal interaction molecule 1 (STIM1) in T_H17 cells leads to reduced expression of genes coding for proteins involved in mitochondrial oxidative phosphorylation (30). Others have reported the role of enhanced mitochondrial oxidative phosphorylation and glycolysis in T_H17 cell differentiation (11, 12), which is consistent with our results of increased expression of markers involved in mitochondrial function, oxidative phosphorylation, and glycolysis in the T_H17 cells. We did find that the switched $Foxp3^+$ T_{reg}-like cells generated under ITK inhibition displayed reduced expression of these markers for mitochondrial function, further emphasizing their altered fate from T_H17 cells.

Altered cellular metabolism changes T cell differentiation fate through the regulation of the mTOR pathway (41, 42), and the inhibition of mTOR in naïve $CD4^+$ T cells prevents the generation of IL-$17A^+$ T_H17 cells and instead leads to the generation of $Foxp3^+$ iT_{reg} cells under T_H17-polarizing conditions (41). In addition, several studies have reported that reduced mTOR signaling induces iT_{reg} differentiation (14, 36, 37), whereas increased mTOR signaling induces T_H17 differentiation (43, 44). Within T_H17 cells, increased mitochondrial function and oxidative phosphorylation mediated by enhanced mTOR signaling induces expression of the T_H17 pioneer transcription factor BATF, allowing maintenance of differentiated T_H17 cells (29). In contrast, deletion of *Batf* in naïve $CD4^+$ T cells increases the expression of Foxp3 even under T_H17-polarizing conditions (29, 45). Our results are consistent with these reports, and further demonstrate that with inhibition of ITK under T_H17-polarizing conditions, the switch in T cell fate from T_H17 to $Foxp3^+$ T_{reg}-like cells similarly involved the mTOR pathway. These results suggest that with ITK inhibition the reduced mitochondrial function, oxidative phosphorylation, and glycolysis, through reduced phosphorylation of mTOR and the mTOR substrate S6K, promoted the switch to $Foxp3^+$ T_{reg}-like cells. Reduced mTOR signaling through the reduced expression of the T_H17 transcription factor BATF is a potential mechanism for the ITK inhibition–dependent switch from T_H17 to $Foxp3^+$ T_{reg}-like cells under T_H17-polarizing conditions.

In conclusion, our results suggest that, under T_H17 conditions, the strong TCR signaling (in the presence of ITK activity) in naïve $CD4^+$ T cells that leads to increased intracellular Ca^{2+} results in enhanced mitochondrial function and oxidative phosphorylation, which can

activate the mTOR pathway to induce the T_H17 transcription factor BATF. In the absence of ITK activity, the reduction in the expression of molecules involved in mitochondrial function and oxidative phosphorylation and subsequent reductions in the activity of the mTOR pathway and BATF expression could act as a potential mechanism for the switch in generating Foxp3$^+$ T_{reg}-like cells instead. The findings of this study provide greater insight into how ITK controls the T_H17 and T_{reg} dichotomy, and these findings could have broader implications for immune disorders with an imbalance of T_H17 and T_{reg}.

MATERIALS AND METHODS

Mice

Male and female mice were on the C57BL/6 background aged between 6 to 8 weeks housed in the specific pathogen free facilities. WT, *Itk*$^{-/-}$ and ITK*as* IL-17A-GFP/Foxp3-RFP dual reporter mouse strains were generated by crossing IL-17A-GFP (B-IL17A-EGFP^{tm1}, Biocytogen, Worchester, MA) with Foxp3-RFP (C57BL/6-*Foxp3*^{tm1Flv}/J, Jackson Laboratory, Bar Harbor, ME) strain (46) as previously reported (16). WT, *Itk*$^{-/-}$ and ITK*as* IL-10-GFP/Foxp3-RFP dual reporter mouse strains were generated as previously described (18). CD45.1 congenic (B6.SJL-*Ptprc*^{a} *Pepc*^{b}) and *Rag1*$^{-/-}$ (B6.129S7-*Rag1*^{tm1Mom}) strains were purchased from Jackson Laboratory. All experiments were performed in accordance with the guidelines established by the Office of Research Protection's Institutional Animal Care and Use Committee at Cornell University.

Flow Cytometry and antibodies

The following antibodies for murine antigens were used labelled as antigen (clone name; catalog number) at a dilution of 1:200 unless indicated otherwise. Viability dye eF506 (65–0866-18) and antibody against CD16/32 (FcBlock) (93; 14016185) were purchased from Thermo Fisher Scientific (Waltham, MA). Antibodies against PD1 (29F.1A12; 135224), pmTOR (pSer2448) (MRRBY, 46971842), CD25 (29F.1A12; 135224), CD4 (GK1.5; 100427), CD45.1 (A20; 110716), CD45.2 (104; 109819), CD3ε (145–2C11; 100340) and CD28 (35.51; 102112) were purchased from Biolegend (San Diego, CA). Antibody against pS6K (pS235/pS236) (N7–548; 561457) was from BD Biosciences (San Jose, CA). Flow cytometry data was generated using the Attune Nxt Flow Cytometer (Thermo Fisher Scientific Waltham, MA) and FACS Aria II (BD, San Jose, CA), which was analyzed using FlowJo (Tree Star, Ashland, OR).

T_H17 and iT_{reg} differentiation in vitro

Naïve CD4$^+$ T cells purified from spleens of WT, *Itk*$^{-/-}$ and ITK*as* IL-17-GFP/Foxp3-RFP dual reporter mice were cocultured with APCs (adherent macrophages and dendritic cells from spleens of *Rag1*$^{-/-}$ mice) for indicated period of days in RPMI media (10% FBS, 0.5% HEPES, 1 mM Glutamine, 1 mM Sodium Pyruvate, 1 mM non-essential amino acids and 100 U/ml Penicillin and Streptomycin). Cells were treated with WT ITK inhibitor CPI-818 (23) (Corvus Pharmaceuticals, Burlingame CA), ITK*as* inhibitor 3MBPP1 (Cayman Chemicals, Ann Arbor, MI), c-Raf inhibitor, p38 inhibitor SB203580, ERK inhibitor SCH772984, JNK inhibitor SP600125, PMA, ionomycin, thapsigarhin, or DMSO were all from Sigma Aldrich. For T_H17 differentiation, naïve CD4$^+$ T cells were

activated by anti-CD3 (2 μg/ml), anti-CD28 (1 μg/ml), in the presence of APCs along with recombinant IL-6 (406-ML-025, 10 ng/ml), recombinant TGF-β (240-B-002, 10 ng/ml), and recombinant human IL-2 protein (202-IL-010), all from R&D Systems (Minneapolis, MN) as described (15). The iT_{reg} cells were generated in vitro by activating coculture of naïve $CD4^+$ T cells with anti-CD3 (1 μg/ml), anti-CD28 (1 μg/ml), recombinant IL-2 (10 μg/ml) and recombinant TGF-β (10 μg/ml) in the presence of APCs. Cells were stained with cell surface markers and/or fixed and permeabilized with the Foxp3/Transcription Factor Staining Kit (eBioscience) with staining for intracellular makers and fixable viability dye eF506 for live/dead cell exclusion to analyze by flow cytometry. Where indicated, cells were also stained with surface markers to sort purify (>95% purity) populations of $CD4^+$ IL-17-GFP^+ T_H17 cells and $CD4^+$ Foxp3-RFP^+ T_{reg}-like cells by BD FACS Aria II.

In vitro suppression assay

$Foxp3^+$ T_{reg}-like cells generated during WT ITK inhibition using CPI-818 under T_H17 conditions, and iT_{reg} cells generated during activation under iT_{reg} conditions, were stained with cell surface markers and sort purified (>95% purity) to obtain $CD4^+$ Foxp3-RFP^+ T_{reg}-like cells and $CD4^+$ Foxp3-RFP^+ iT_{reg} cells. Sort-purified naïve responding $CD4^+$ T cells were labelled with CFSE proliferation dye (Invitrogen) and cocultured with $Foxp3^+$ T_{reg}-like cells or iT_{reg} cells in presence of anti-CD3 (1 μg/ml) for 3 days, followed by analysis of CFSE dye dilution using flow cytometry.

HDM-induced allergic airway inflammation

WT, *Itk*$^{-/-}$ and ITK*as* IL-17-GFP/Foxp3-RFP dual reporter mice were anaesthetized with isoflurane and exposed intranasally to HDM extract (10 μg once daily, *Dermatophagoides pteronyssinus,* Greer Laboratories, Lenoir, NC) for 10 days as previously described (26), followed by treatment with ITK inhibitor CPI-818 (50 mg/kg/day once daily by oral gavage, Corvus Pharmaceuticals, Burlingame, CA) or vehicle control while maintaining HDM (10 μg once daily) exposure for a further 10 day period. Mice were then euthanized and lung tissue collected for cytometric analysis. The number of mice used is indicated in the legend of the appropriate figure. Sample size was determined by power analysis.

RNA- and ATAC-Sequencing

Total RNA was extracted from sort purified T_H17, $Foxp3^+$ T_{reg}-like cells generated in vitro from WT naïve $CD4^+$ T cells and iT_{reg} cells using TRIzol reagent (Invitrogen). The RNA library was generated using the NEB Ultra II Directional RNA Library Prep Kit and quantified using Qubit Bioanalyzer. RNA sequencing was performed on an Illumina NextSeq500 at 75bp reads and 20 million reads per sample (Transcriptional Regulation and Expression Facility (TREx), Cornell University) as previously described (47). RNA sequencing data was demultiplexed by BCL2FASTQ2 and FASTQC performed. RNA-Seq data was mapped to the mm10 genome using STAR aligner and raw counts obtained using HTSeq. Counts were normalized and differentially expressed genes identified using DESeq2 (FDR<0.05). Gene set enrichment analysis (GSEA) was performed using software developed by the Broad Institute (48, 49) and heat map generated using R Studio (Boston, MA) and Heatmapper (50). Data was compared to published RNA-Seq data from Gene

Expression Omnibus repository (GEO) dataset GSE158703 with the indicated T_H cell subsets.

For ATAC-Seq, T_H17, Foxp3$^+$ T_{reg}-like cells and iT_{reg} cells generated in vitro were sort purified and frozen in 10% DMSO in cell culture media. Nuclei were permeabilized (10 mM Tris-HCl, pH 8.0, 10 mM NaCl, 2 mM Mg Acetate) and lysed (10 mM Tris-HCl, pH 8.0, 10 mM NaCl, 2 mM Mg Acetate, 6 mM CaCl2, 0.2% Ipegal, 0.016% Tween20, 600 mM Sucrose) as per instructions from the TREx facility at Cornell University. The lysed nuclei were provided to the TREx facility for transposition reaction (47). DNA library generated was quantified using Qubit BioAnalyzer and sequencing performed on an Illumina NextSeq500 at 75bp reads and 20 million reads per sample followed by FASTQC analysis for quality control. ATAQ-Seq data was aligned to mm10 genome using Bowtie, ATAC-Seq peaks were identified by MACS2, and promoter region associated peaks were identified by bedtools as described in (51), by the TREx facility. Analysis was performed in R Studio (Boston, MA) and using the UCSC genome browser (University of California at Santa Cruz). The RNA sequencing and ATAC-Seq data has been deposited in National Center for Biotechnology Information (NCBI) GEO repository with the accession numbers GSE261352 and GSE266002 respectively.

Statistical analysis

Data were examined for statistical significance using GraphPad Prism (San Diego, CA), using Students T test with Welch's correction, or One way ANOVA with Holm-Sidak's post hoc analysis for multiple comparison between samples, with *$p \leq 0.05$, **$p \leq 0.005$, ***$p \leq 0.001$ and ****$p \leq 0.0001$ considered as statistically significant. SEM values are plotted in relevant figures, but in some cases may not be apparent due to size of the symbols in the plots.

Supplementary Material

Refer to Web version on PubMed Central for supplementary material.

Acknowledgments:

We thank Amie Redko for animal care, members in the August lab for comments and feedback, Dr. James Janc (Corvus Pharmaceuticals) for CPI-818, and Dr. Jen Grenier of the RNA Sequencing Core for guidance.

Funding:

This work was supported in part by grants from: The National Institutes of Health (AI120701) to AA.

The National Institutes of Health (AI138570) to AA.

The National Institutes of Health (AI129422) to AA and WH.

The National Institutes of Health to The RNA Sequencing Core (U54 HD076210) HHMI Professorship to AA.

References and Notes

1. Belizario JE, Brandao W, Rossato C, Peron JP, Thymic and Postthymic Regulation of Naive CD4(+) T-Cell Lineage Fates in Humans and Mice Models. Mediators Inflamm 2016, 9523628 (2016). [PubMed: 27313405]
2. Tuzlak S et al. , Repositioning T. Nat Immunol 22, 1210–1217 (2021). [PubMed: 34545250]
3. Bhattacharyya ND, Feng CG, Regulation of T Helper Cell Fate by TCR Signal Strength. Front Immunol 11, 624 (2020). [PubMed: 32508803]
4. Diller ML, Kudchadkar RR, Delman KA, Lawson DH, Ford ML, Balancing Inflammation: The Link between TH17 and Regulatory T Cells. Mediators Inflamm 2016, 6309219 (2016). [PubMed: 27413254]
5. Fang D, Healy A, Zhu J, Differential regulation of lineage-determining transcription factor expression in innate lymphoid cell and adaptive T helper cell subsets. Front Immunol 13, 1081153 (2022). [PubMed: 36685550]
6. Noack M, Miossec P, T_H17 and regulatory T cell balance in autoimmune and inflammatory diseases. Autoimmun Rev 13, 668–677 (2014). [PubMed: 24418308]
7. Smith-Garvin JE, Koretzky GA, Jordan MS, T Cell Activation. Annual Review of Immunology 27, 591–619 (2009).
8. Andreotti AH, Schwartzberg PL, Joseph RE, Berg LJ, T-cell signaling regulated by the Tec family kinase, Itk. Cold Spring Harb Perspect Biol 2, a002287 (2010). [PubMed: 20519342]
9. Kannan A, Huang WS, Huang F, August A, Signal transduction via the T cell antigen receptor in naive and effector/memory T cells. International Journal of Biochemistry & Cell Biology 44, 2129–2134 (2012). [PubMed: 22981631]
10. Barbi J, Pardoll D, Pan F, Metabolic control of the T_{reg}/T_H17 axis. Immunol Rev 252, 52–77 (2013). [PubMed: 23405895]
11. Wagner A et al. , Metabolic modeling of single T_H17 cells reveals regulators of autoimmunity. Cell 184, 4168–4185.e4121 (2021). [PubMed: 34216539]
12. Michalek RD et al. , Cutting edge: distinct glycolytic and lipid oxidative metabolic programs are essential for effector and regulatory $CD4^+$ T cell subsets. J Immunol 186, 3299–3303 (2011). [PubMed: 21317389]
13. Miller AT, Wilcox HM, Lai ZB, Berg LJ, Signaling through ltk promotes T helper 2 differentiation via negative regulation of T-bet. Immunity 21, 67–80 (2004). [PubMed: 15345221]
14. Gomez-Rodriguez J et al. , Itk-mediated integration of T cell receptor and cytokine signaling regulates the balance between TH17 and regulatory T cells. Journal of Experimental Medicine 211, 529–543 (2014). [PubMed: 24534190]
15. Gomez-Rodriguez J et al. , Differential Expression of Interleukin-17A and-17F Is Coupled to T Cell Receptor Signaling via Inducible T Cell Kinase. Immunity 31, 587–597 (2009). [PubMed: 19818650]
16. Kannan A et al. , Allele-sensitive mutant, Itk as, reveals that Itk kinase activity is required for T_H1, T_H2, T_H17, and iNKT-cell cytokine production. Eur J Immunol 45, 2276–2285 (2015). [PubMed: 25989458]
17. Huang WS, Jeong AR, Kannan AK, Huang L, August A, IL-2-Inducible T Cell Kinase Tunes T Regulatory Cell Development and Is Required for Suppressive Function. Journal of Immunology 193, 2267–2272 (2014).
18. Huang WS, Solouki S, Koylass N, Zheng SG, August A, ITK signalling via the Ras/IRF4 pathway regulates the development and function of Tr1 cells. Nature Communications 8, (2017).
19. Elmore JP et al. , Tuning T helper cell differentiation by ITK. Biochem Soc Trans 48, 179–185 (2020). [PubMed: 32049330]
20. Sahu N, August A, ITK inhibitors in inflammation and immune-mediated disorders. Curr Top Med Chem 9, 690–703 (2009). [PubMed: 19689375]
21. Vargas L, Hamasy A, Nore BF, Smith CI, Inhibitors of BTK and ITK: state of the new drugs for cancer, autoimmunity and inflammatory diseases. Scand J Immunol 78, 130–139 (2013). [PubMed: 23672610]

22. Lin TA et al. , Selective Itk inhibitors block T-cell activation and murine lung inflammation. Biochemistry 43, 11056–11062 (2004). [PubMed: 15323564]
23. Janc JW et al. , CPI-818: A selective inhibitor of interleukin-2-inducible T-cell kinase (ITK) that inhibits T-cell receptor signaling, promotes TH1 skewing, and achieves objective tumor responses when administered to dogs with T cell lymphomas. Cancer Research 79, 2 (2019).
24. ClinicalTrails.gov. (2021).
25. Khodadoust MS et al. , Cpi-818, an Oral Interleukin-2-Inducible T-Cell Kinase Inhibitor, Is Well-Tolerated and Active in Patients with T-Cell Lymphoma. Blood 136, 19–20 (2020).
26. Kannan A, Sahu N, Mohanan S, M. S., A. August, Itk modulates allergic airway inflammation by suppressing IFNγ in naïve $CD4^+$ T-cells. J. Allergy Clin. Immunol. 132, 811–820.e811-815. (2013). [PubMed: 23768572]
27. Zhang H et al. , An IL-27-Driven Transcriptional Network Identifies Regulators of IL-10 Expression across T Helper Cell Subsets. Cell Rep 33, 108433 (2020). [PubMed: 33238123]
28. Roose J, Mollenauer M, Gupta V, Stone J, Weiss A, A diacylglycerol-protein kinase C-RasGRP1 pathway directs Ras activation upon antigen receptor stimulation of T cells. Mol Cell Biol. 25, 4426–4441. (2005). [PubMed: 15899849]
29. Shin B et al. , Mitochondrial Oxidative Phosphorylation Regulates the Fate Decision between Pathogenic T_H17 and Regulatory T Cells. Cell Rep 30, 1898–1909.e1894 (2020). [PubMed: 32049019]
30. Kaufmann U et al. , Calcium Signaling Controls Pathogenic T_H17 Cell-Mediated Inflammation by Regulating Mitochondrial Function. Cell Metabolism 29, 1104-+ (2019). [PubMed: 30773462]
31. Kannan AK, Kim DG, August A, Bynoe MS, Itk signals promote neuroinflammation by regulating $CD4^+$ T-cell activation and trafficking. J Neurosci 35, 221–233 (2015). [PubMed: 25568116]
32. Kitagawa Y, Ohkura N, Sakaguchi S, Molecular determinants of regulatory T cell development: the essential roles of epigenetic changes. Front Immunol 4, 106 (2013). [PubMed: 23675373]
33. Miyara M et al. , Functional delineation and differentiation dynamics of human $CD4^+$ T cells expressing the FoxP3 transcription factor. Immunity 30, 899–911 (2009). [PubMed: 19464196]
34. Wei G et al. , Global mapping of H3K4me3 and H3K27me3 reveals specificity and plasticity in lineage fate determination of differentiating $CD4^+$ T cells. Immunity 30, 155–167 (2009). [PubMed: 19144320]
35. Miskov-Zivanov N, Turner MS, Kane LP, Morel PA, Faeder JR, The duration of T cell stimulation is a critical determinant of cell fate and plasticity. Sci Signal 6, ra97 (2013). [PubMed: 24194584]
36. Sauer S et al. , T cell receptor signaling controls Foxp3 expression via PI3K, Akt, and mTOR. Proc Natl Acad Sci U S A 105, 7797–7802 (2008). [PubMed: 18509048]
37. Hawse WF, Boggess WC, Morel PA, TCR Signal Strength Regulates Akt Substrate Specificity To Induce Alternate Murine T_H and T Regulatory Cell Differentiation Programs. J Immunol 199, 589–597 (2017). [PubMed: 28600288]
38. Wang X et al. , Calmodulin and $PI(3,4,5)P_3$ cooperatively bind to the Itk pleckstrin homology domain to promote efficient calcium signaling and IL-17A production. Sci Signal 7, ra74 (2014). [PubMed: 25097034]
39. Dolmetsch RE, Lewis RS, Goodnow CC, Healy JI, Differential activation of transcription factors induced by Ca^{2+} response amplitude and duration. Nature 386, 855–858 (1997). [PubMed: 9126747]
40. Dolmetsch RE, Xu K, Lewis RS, Calcium oscillations increase the efficiency and specificity of gene expression. Nature 392, 933–936 (1998). [PubMed: 9582075]
41. Shi LZ et al. , HIF1alpha-dependent glycolytic pathway orchestrates a metabolic checkpoint for the differentiation of T_H17 and T_{reg} cells. J Exp Med 208, 1367–1376 (2011). [PubMed: 21708926]
42. Dang EV et al. , Control of T(H)17/T(reg) balance by hypoxia-inducible factor 1. Cell 146, 772–784 (2011). [PubMed: 21871655]
43. Delgoffe GM et al. , The kinase mTOR regulates the differentiation of helper T cells through the selective activation of signaling by mTORC1 and mTORC2. Nat Immunol 12, 295–303 (2011). [PubMed: 21358638]

44. Kastirr I et al. , Signal Strength and Metabolic Requirements Control Cytokine-Induced T_H17 Differentiation of Uncommitted Human T Cells. J Immunol 195, 3617–3627 (2015). [PubMed: 26378072]
45. Schraml BU et al. , The AP-1 transcription factor Batf controls T(H)17 differentiation. Nature 460, 405–409 (2009). [PubMed: 19578362]
46. Wan YSY, Flavell RA, Identifying Foxp3-expressing suppressor T cells with a bicistronic reporter. Proceedings of the National Academy of Sciences of the United States of America 102, 5126–5131 (2005). [PubMed: 15795373]
47. Elmore J et al. , ITK independent development of TH17 responses during hypersensitivity pneumonitis driven lung inflammation. Commun Biol 5, 162 (2022). [PubMed: 35210549]
48. Mootha VK et al. , PGC-1 alpha-responsive genes involved in oxidative phosphorylation are coordinately downregulated in human diabetes. Nat Genet 34, 267–273 (2003). [PubMed: 12808457]
49. Subramanian A et al. , Gene set enrichment analysis: a knowledge-based approach for interpreting genome-wide expression profiles. Proc Natl Acad Sci U S A 102, 15545–15550 (2005). [PubMed: 16199517]
50. Babicki S et al. , Heatmapper: web-enabled heat mapping for all. Nucleic Acids Res 44, W147–153 (2016). [PubMed: 27190236]
51. Corces MR et al. , An improved ATAC-seq protocol reduces background and enables interrogation of frozen tissues. Nat Methods 14, 959–962 (2017). [PubMed: 28846090]

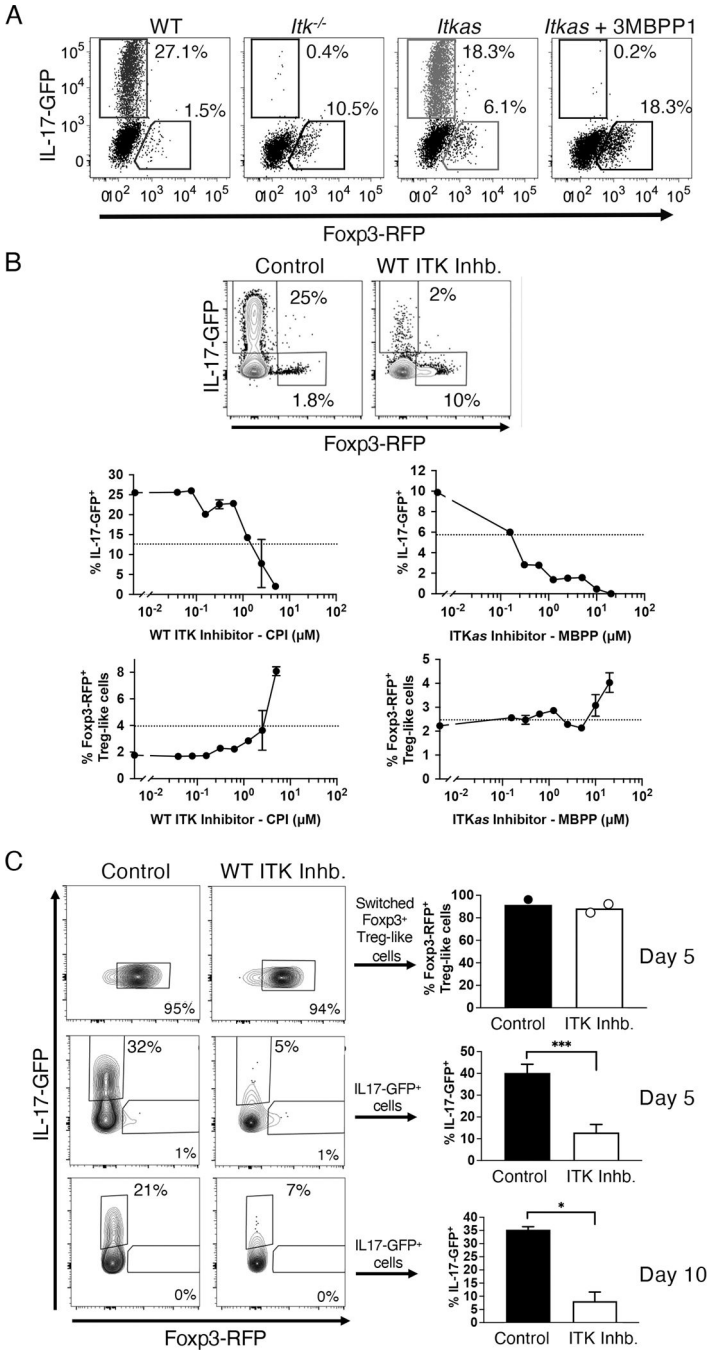

Fig. 1. Loss or inhibition of ITK causes naïve CD4$^+$ T cells activated under T$_H$17-inducing conditions to differentiate into Foxp3$^+$ T$_{reg}$-like cells.

(**A**) Naïve WT, *Itk*$^{-/-}$, or ITK*as* IL-17A-GFP/Foxp3-RFP CD4$^+$ T cells were activated under T$_H$17 differentiation conditions in the presence of the ITK*as* inhibitor 3MBPP1 or DMSO control, followed by flow cytometric analysis of IL-17A-GFP and Foxp3-RFP. Data are representative of n = 3 independent experiments. (**B**) Naïve WT IL-17A-GFP/Foxp3-RFP CD4$^+$ T cells were activated under T$_H$17 differentiation conditions in the presence of CPI-818, an inhibitor of WT ITK (WT ITK Inhb), or DMSO (control), followed by flow

cytometric analysis for IL-17A-GFP and Foxp3-RFP. The graphs show the percentages of IL-17A-GFP$^+$ cells and Foxp3-RFP$^+$ T_{reg}-like cells after naïve WT (left) or ITK*as* (right) IL-17A-GFP/Foxp3-RFP CD4$^+$ T cells were activated under T_H17 differentiation conditions in the presence of CPI-818 (CPI) or 3MBPP1 (MBPP) or DMSO control (0 μM inhibitor). Mean ± SEM. Data are representative of n = 3 independent experiments. (**C**) Switched Foxp3$^+$ T_{reg}-like cells generated under T_H17 differentiation conditions in the presence of CPI-818 or in vitro–generated T_H17 cells were reactivated under T_H17 differentiation conditions in the presence of CPI-818 or DMSO (control) for 5 days (switched Foxp3$^+$ T_{reg}-like cells, and T_H17 cells) or 10 days (T_H17 cells), followed by flow cytometric analysis for IL-17A-GFP and Foxp3-RFP. n = 2 independent experiments (switched Foxp3$^+$ T_{reg}-like cells), n = 3 independent experiments (T_H17 cells for 5 and 10 days). Mean ± SEM. All data were analyzed for statistical significance using Student's T test with Welch's correction where * $p \leq 0.05$, ** $p \leq 0.005$.

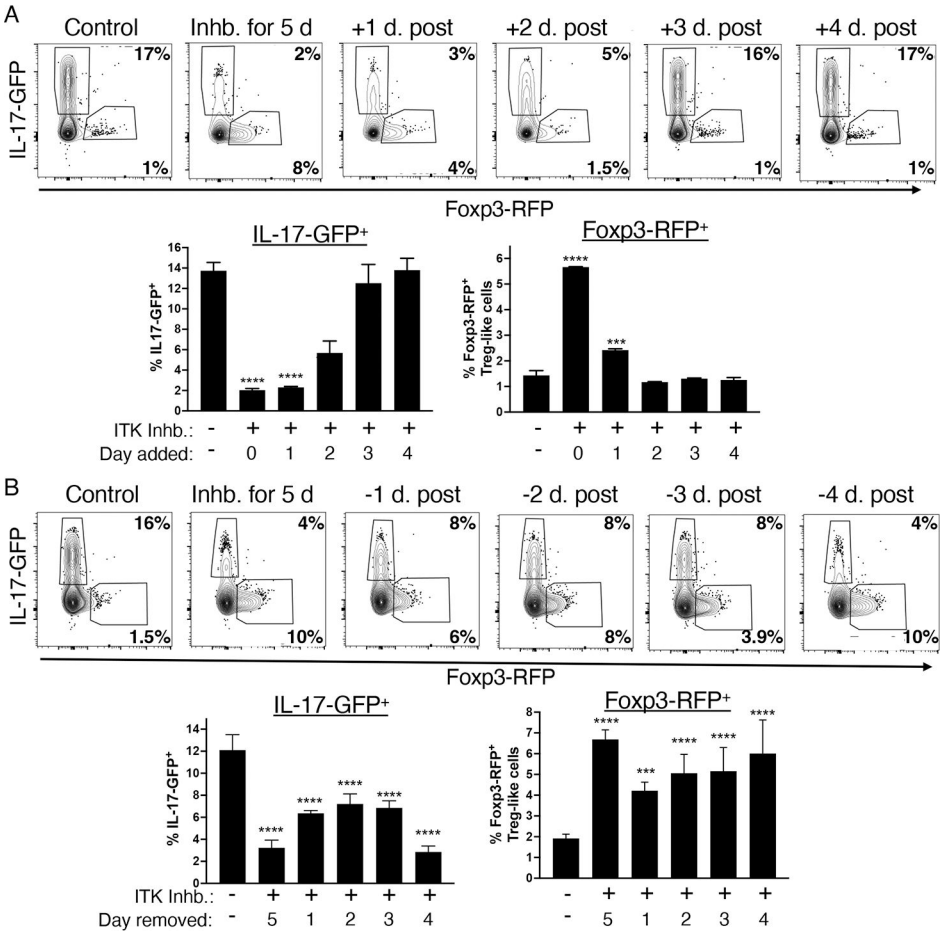

Fig. 2. Loss of ITK activity during the early phases of activation switches differentiation from T_H17 to Foxp3$^+$ T_{reg}-like cells.

(**A**) Naïve WT IL-17A-GFP/Foxp3-RFP CD4$^+$ T cells were activated under T_H17 differentiation conditions (control) and treated with the ITK inhibitor CPI-818 (ITK Inhb) for 5 days, or the inhibitor was added after 1, 2, 3 or 4 days of activation. The cells were analyzed by flow cytometry for IL-17A-GFP and Foxp3-RFP on day 5. n = 3 independent experiments. (**B**) Naïve WT IL-17A-GFP/Foxp3-RFP CD4$^+$ T cells were activated under T_H17 differentiation conditions (control) in the presence of CPI-818 for 5 days, or the inhibitor was removed after 1, 2, 3 or 4 days of activation. Flow cytometric analysis for IL-17A-GFP and Foxp3-RFP was done on day 5. n = 3 independent experiments. Mean ± SEM, one-way ANOVA (which was significant at $p<0.0001$), with Holm-Sidak's multiple comparison test for statistical significance. * $p \leq 0.05$, ** $p \leq 0.005$, *** $p \leq 0.001$ and **** $p \leq 0.0001$.

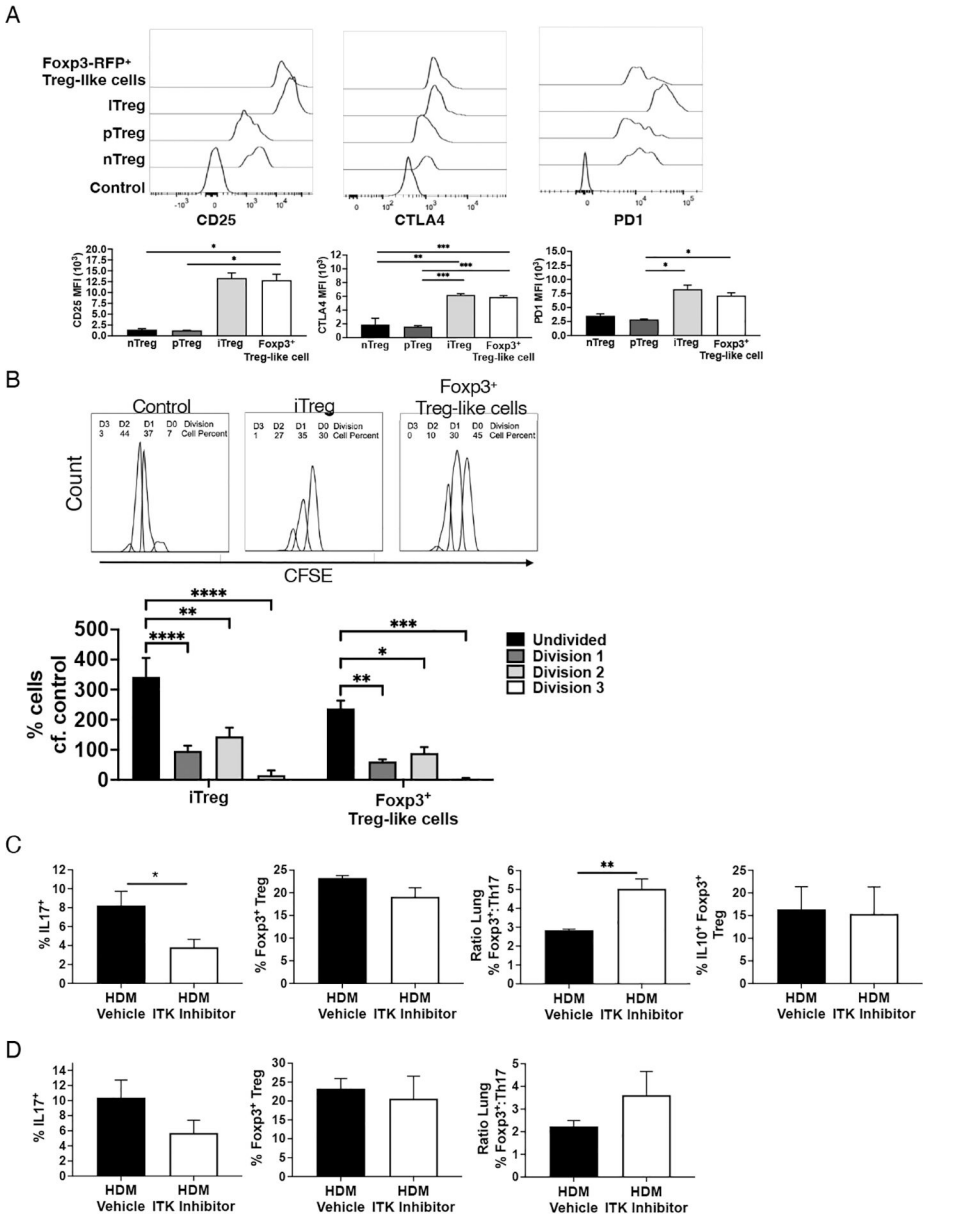

Fig. 3. ITK inhibition functionally switches Foxp3$^+$ T_{reg}-like cells and alters the Foxp3$^+$ T_{reg}:T_H17 cell ratio in lungs during HDM-induced allergic airway inflammation.

(**A**) Foxp3$^+$ T_{reg}-like cells generated from WT IL-17A-GFP/Foxp3-RFP naïve CD4$^+$ T cells were activated under T_H17 differentiation conditions in the presence of ITK inhibitor CPI-818 and compared to iT_{reg} cells, pT_{reg} cells, and nT_{reg} cells for expression of the indicated T_{reg} markers. Control, naïve CD4$^+$ T cells. MFI, mean fluorescence intensity. Mean ± SEM. One-way ANOVA (significant at $p<0.005$) with Holm-Sidak's multiple comparison test for statistical significance. n = 3 (nT_{reg} cells), n = 3 (pT_{reg} cells), n = 8 (iT_{reg} cells), or n = 56 (Foxp3$^+$ T_{reg}-like cells) independent experiments. (**B**) CD45.2$^+$ switched Foxp3$^+$ T_{reg}-like cells generated in the presence of CPI-818 under T_H17 conditions and iT_{reg}cells were sort-purified, followed by coculture with CFSE-labelled CD45.1 naïve CD4$^+$ T cell responders for 3 days. Representative CFSE plots and quantification of the

percentage suppression naïve $CD4^+$ T cell responder proliferation by $Foxp3^+$ T_{reg}-like cells and iT_{reg} cells are shown. n = 4 independent experiments. Mean ± SEM for percentage of cells undergoing division. One-way ANOVA with Holm-Sidak's multiple comparison test for statistical significance. (**C and D**) WT (C) or ITK*as* (D) IL-17A-GFP/Foxp3-RFP mice were exposed intranasally to HDM extract for 10 days, followed by a second round of 10 day intranasal exposure to HDM extract, along with treatment with CPI-818 (ITK Inhibitor) or vehicle. Lung cells were analyzed by flow cytometry for IL-17A-GFP and Foxp3-RFP the determine percent T_H17s, percent $Foxp3^+$ T_{reg} cells, ratio percent $Foxp3^+$:T_H17 cells, and percent IL-10^+Foxp3^+ T cells. n=6 (WT) or 4 (ITK*as*) mice per group. Mean ± SEM, Student's T test with Welch's correction for statistical significance. For all data, * $p \leq 0.05$, ** $p \leq 0.005$, *** $p \leq 0.001$ and **** $p \leq 0.0001$.

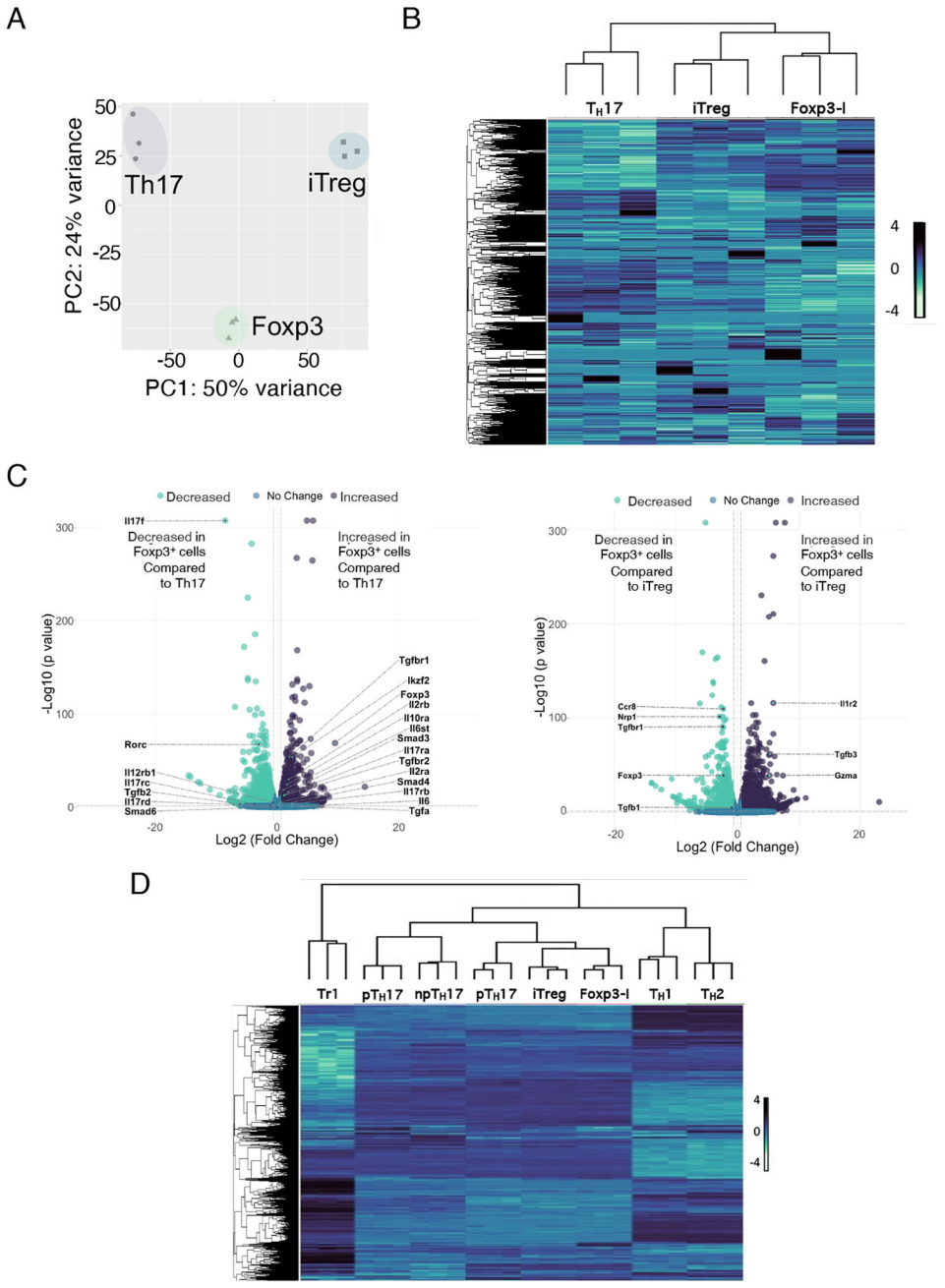

Fig. 4. The transcriptomic profile of ITK inhibition–induced switched Foxp3$^+$ T$_{reg}$-like cells is similar to that of iT$_{reg}$ cells.

The transcriptomes of switched Foxp3$^+$ T$_{reg}$-like cells and in vitro–generated T$_H$17s and iT$_{reg}$ cells were compared by RNA-Seq analysis. (**A**) PCA analysis, (**B**) heatmap of global gene expression, and **(C**) volcano plots of differentially expressed genes are shown. n = 3 samples pooled from multiple mice for each subset. (**D**) The transcriptome of switched Foxp3$^+$ T$_{reg}$-like cells were compared by heatmap with the published transcriptomes of Tr1, pT$_H$17, npT$_H$17, T$_H$1 and T$_H$2 cells (GSE158703).

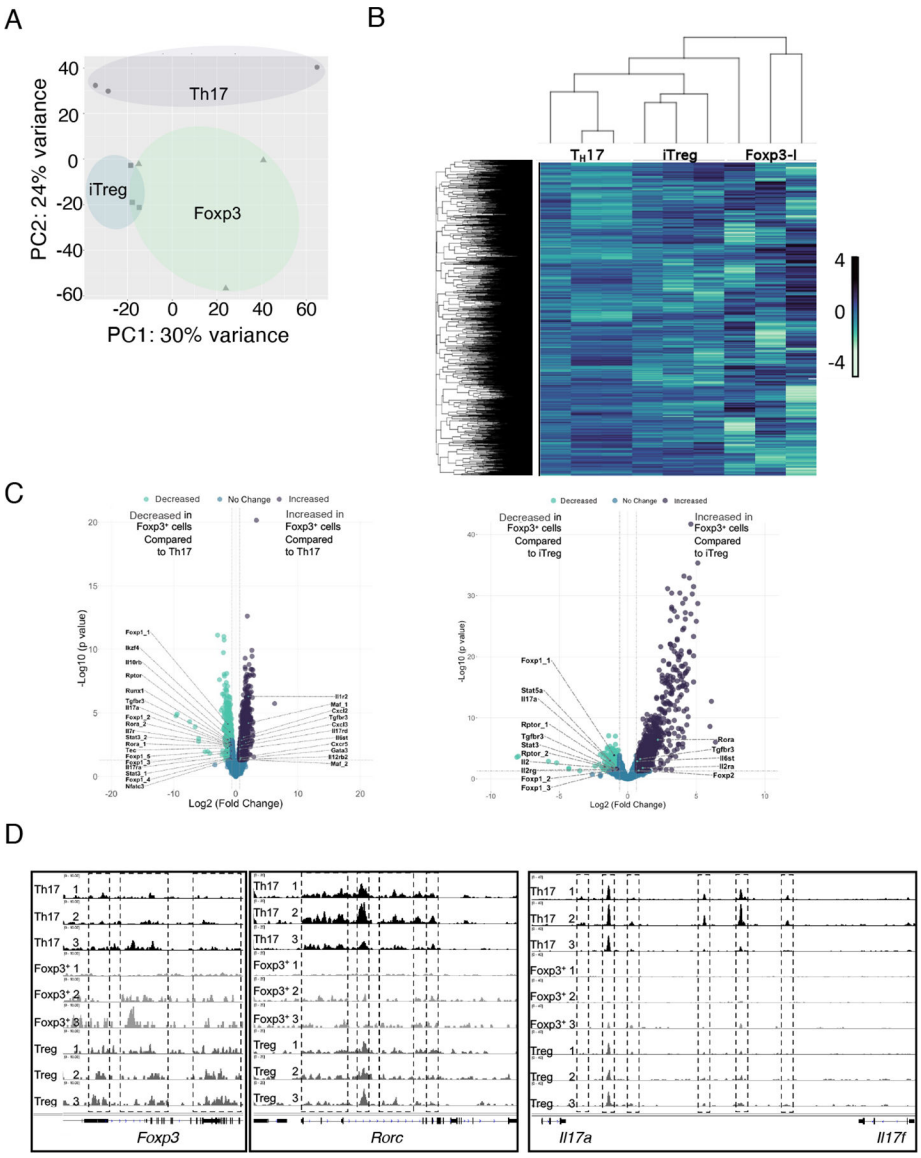

Fig. 5. The chromatin accessibility profile of ITK inhibition–induced switched Foxp3$^+$ T$_{reg}$-like cells is distinct from that of T$_H$17 and iT$_{reg}$ cells.

Switched Foxp3$^+$ T$_{reg}$-like cells, and in vitro–generated T$_H$17 and iT$_{reg}$ cells were analyzed by ATAC-Seq. (**A**) PCA analysis, (**B**) heatmap of global differential peaks in chromatin accessibility, and (**C**) fold changes of global differential peaks in chromatin accessibility are shown. (**D**) Tracks indicating areas of chromatin accessibility for *Foxp3*, *Rorc*, *Il17a*, and *Il17f* in switched Foxp3$^+$ T$_{reg}$-like cells, T$_H$17 cells, and iT$_{reg}$ cells. n = 3 samples pooled from multiple mice for each subset.

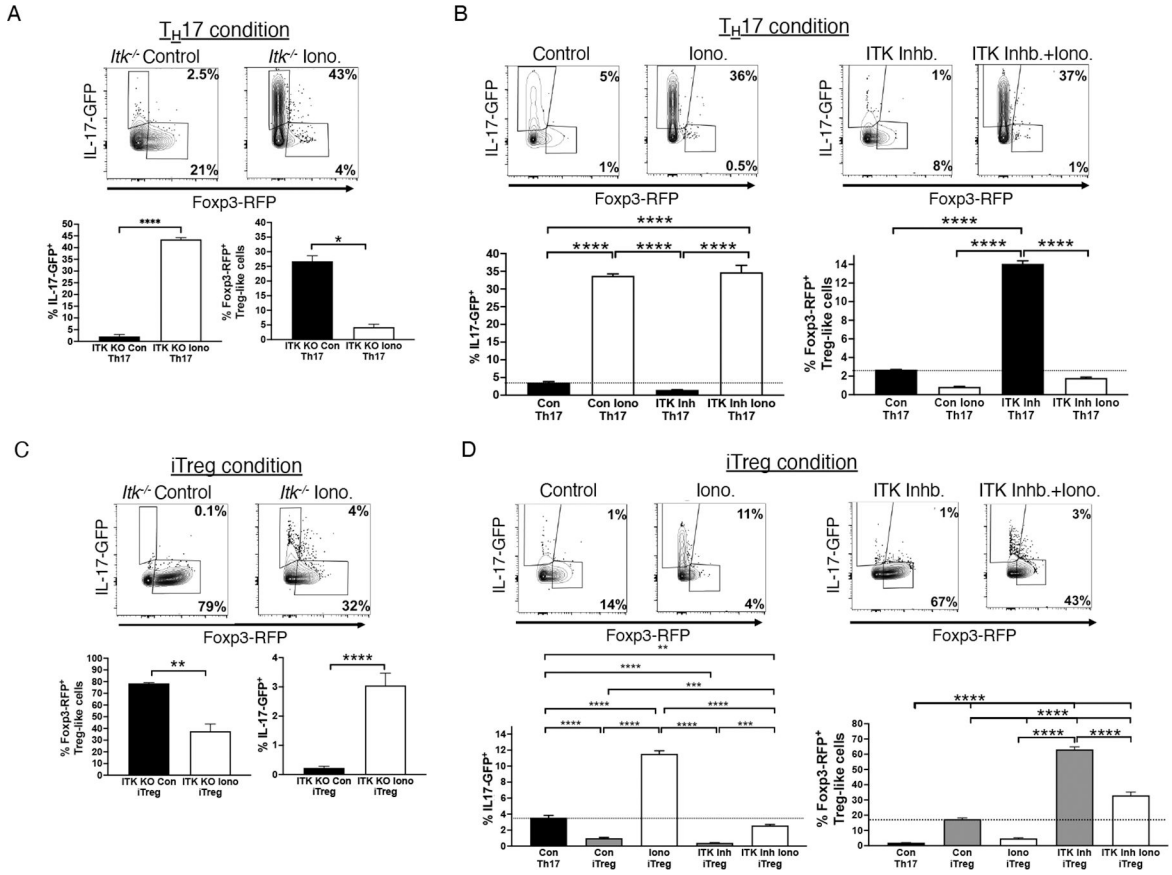

Fig. 6. Enhancing Ca^{2+} signaling prevents the switch to $Foxp3^+$ T_{reg}-like cells when ITK is inhibited.

(**A and B**) Naïve *Itk*$^{-/-}$ (A) or WT (B) IL-17A-GFP/Foxp3-RFP $CD4^+$ T cells were activated under T_H17 differentiation conditions in the presence of ionomycin (Iono) or DMSO (control), with or without the ITK inhibitor CPI-818 (ITK Inhb) as indicated. Cells were analyzed by flow cytometry for IL-17A-GFP and Foxp3-RFP. Representative flow plots and quantification are shown. n = 4 (A) or 3 (B) independent experiments using cells pooled from multiple mice. (**C and D**) Naïve *Itk*$^{-/-}$ (C) or WT (D) IL-17A-GFP/Foxp3-RFP $CD4^+$ T cells were activated under iT_{reg} differentiation conditions in the presence of ionomycin or DMSO, with or without CPI-818 as indicated, followed by flow cytometric analysis of IL-17A-GFP and Foxp3-RFP. Representative flow plots and quantification are shown. n = 4 (C) or 3 (D) independent experiments using cells pooled from multiple mice. Mean ± SEM, (A, C) Student's T test with Welch's correction and (B, D) one way ANOVA (significant at $p<0.0005$) with Holm-Sidak's multiple comparison test for statistical significance. * $p \leq 0.05$, ** $p \leq 0.005$, *** ≤ p 0.001 and **** $p \leq 0.0001$.

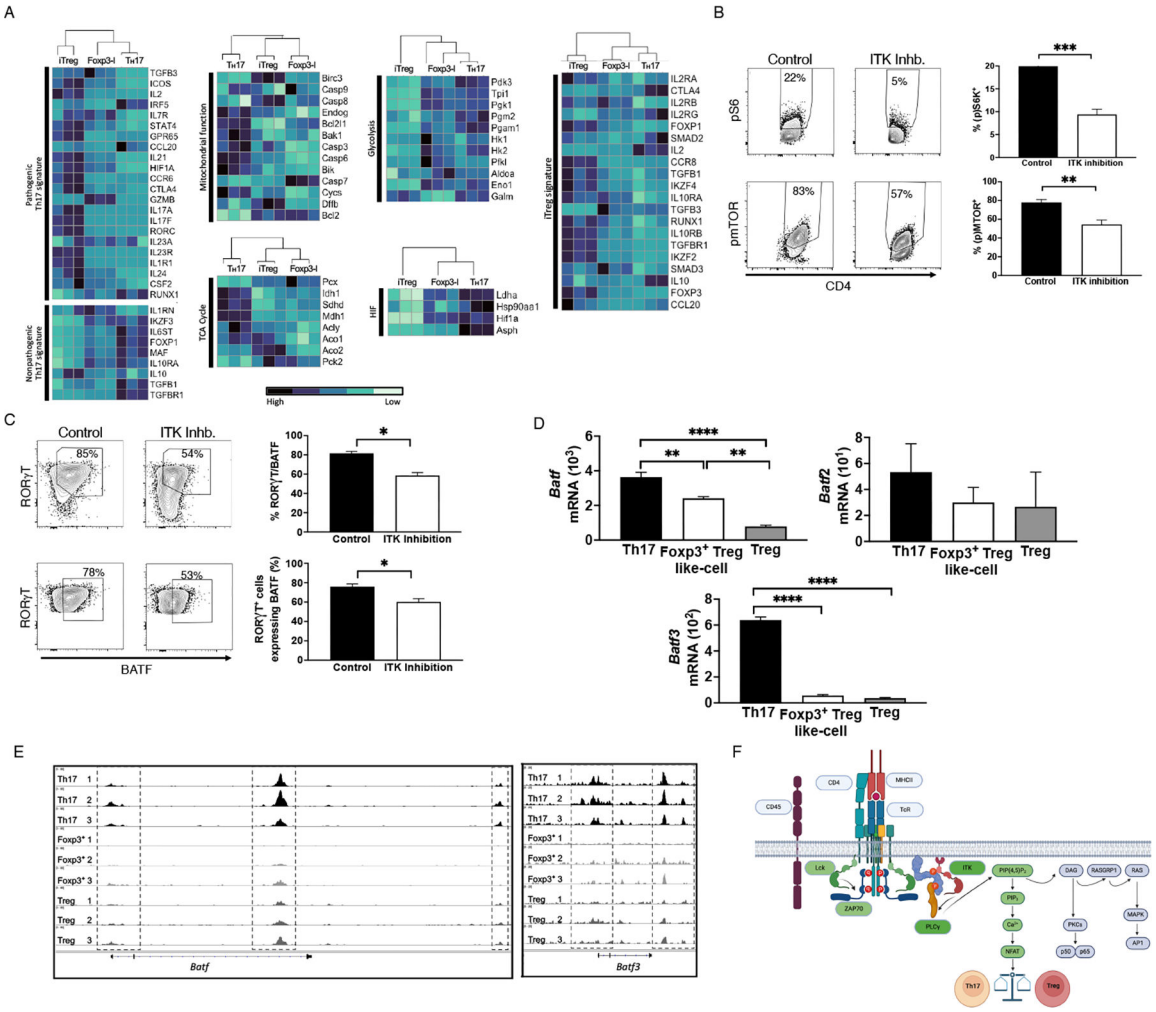

Fig. 7. ITK inhibition–induced Foxp3$^+$ T_{reg}-like cell switching is characterized by changes in metabolic pathways and BATF expression.

(**A**) Heat map of signature genes associated with pathogenic or non-pathogenic T_H17 cells, involved in metabolic changes associated with T_H17 differentiation (the TCA cycle, mitochondrial function, HIF1α, and glycolysis), or associated with iT_{reg} cells in the transcriptomes of switched Foxp3$^+$ T_{reg}-like cells, T_H17 cells, and iT_{reg} cells. n = 3 independent experiments using pooled cells from multiple mice. (**B**) Naïve CD4$^+$ T cells activated under T_H17 differentiation conditions in the presence or absence of the ITK inhibitor CPI-818 (ITK Inhb) were analyzed for phosphorylation of S6K and mTOR by flow cytometry. n = 5 independent experiments. Mean ± SEM, with T test for statistical significance. (**C**) Naïve CD4$^+$ T cells activated under T_H17 differentiation conditions in the presence or absence of CPI-818 were analyzed for BATF and RORγt by flow cytometry (top), or gated on RORγt$^+$ cells and then analyzed for RORγt and BATF (bottom). n = 4 independent experiments. Mean ± SEM, with T test for statistical significance. (**D**) Quantification of *Batf*, *Batf2*, and *Batf3* transcripts (as FPKM, fragments per kilobase million) in switched Foxp3$^+$ T_{reg}-like, T_H17, and iT_{reg} cells. n = 3 samples pooled from multiple mice for each subset. Mean ± SEM, one way ANOVA (significant at $p<0.0001$) with Holm-Sidak's multiple comparison test was performed for statistical significance. (**E**)

Plot of chromatin accessibility for *Batf* in switched Foxp3^{+} T_{reg}-like cells, T_H17 and iT_{reg} cells., n = 3 samples pooled from multiple mice for each subset. For all data, * $p \leq 0.05$, ** $p \leq 0.005$, *** $p \leq 0.001$, **** $p \leq 0.0001$. (**F**) Proposed model of TCR signaling through ITK that triggers increased intracellular Ca^{2+} (in green), but not the Ras/MAPK pathway (grey), leading to balance between T_H17 and T_{reg} cells.